

Low energy acetone dimer ion/surface collisions studied with high energy resolution

C. Mair¹, T. Fiegele¹, F. Biasioli¹, and T.D. Märk^{1,2}

¹Institut für Ionenphysik, Leopold Franzens Universität, Technikerstr. 25, A-6020 Innsbruck, Austria

²Dept. Plasmaphysics, Univerzita Komenskeho, Mlynska dolina, SK-842 15 Bratislava 4, Slovensko

Received: 2 September 1998 / Received in final form: 14 January 1999

Abstract. We have recently constructed the tandem mass spectrometer set-up BESTOF (consisting of a B-sector field combined with an E-sector field, a Surface and a Time Of Flight mass spectrometer) which allows the investigation of ion/surface reactions with high primary mass and energy resolution. Using BESTOF we have extended previous investigations from molecular projectile ions to cluster ions. In particular, we have studied here surface induced dissociation (SID) and surface induced reactions (SIR) of acetone dimer ions upon impact on a hydrocarbon covered stainless steel surface as a function of incident collision energy up to about 80 eV.

PACS. 34.90.+q Other topics in atomic and molecular collision processes and interactions – 82.65.Fr Film and membrane processes: ion exchange, dialyse, osmosis, electroosmosis – 82.30.Fi Ion–molecule, ion–ion, and charge transfer reactions

1 Introduction

Ion surface (reactive) collisions is a research area which is rapidly growing in an effort to identify and explore new methods for both characterizing gaseous ions and the nature of the surface [1, 2]. Besides physical and chemical sputtering the following processes have been identified and investigated in the past years for collisions in the range of tens of eV laboratory energy: (1) reflection, (2) surface induced dissociation (SID), (3) charge exchange reactions (CER) and (4) surface induced reactions (SIR).

In addition of being of fundamental importance, polyatomic ion-surface reactions are also relevant to technological applications [2] encompassing such diverse fields as (i) secondary ion mass spectrometry, (ii) reactive scattering for surface analysis, (iii) surface-induced dissociation for structural analysis, (iv) surface modifications for the preparation of new electronic materials (including the large area of plasma processing) and, quite importantly, (v) plasma-wall interactions in electrical discharges and fusion plasmas [3]. For example, dielectric etching using fluorocarbon plasmas [4] is a major tool in the integrated circuit (IC) manufacturing industry. Models of low-temperature, nonequilibrium plasmas, in particular for the description of the physical phenomena, have developed rapidly [5]. However, lack of fundamental data for the most important species is the single largest factor limiting the successful application of such models to emerging problems of industrial interest [5]. A similar situation exists for data concerning plasma wall interactions of relevance to the plasma edge of fusion tokamaks [3, 6].

A particular interesting and exciting sub-field in the area of ion surface collisions is the interaction of clusters with surfaces [7]. Whereas cluster science has developed in the past two decades to a well established field in physics and chemistry (see for instance an early review in 1984 summarizing the pioneering years [8] as compared to a recent textbook on the same subject [9]), recently a novel and potentially very useful area has emerged, i.e., the interaction of neutral or ionized clusters with surfaces [7] including a large variety of atomically clean or adsorbate covered, polycrystalline or single crystal surfaces. Depending on the initial kinetic energy of the impinging cluster projectile the interaction with a surface leads either to cluster deposition, to cluster fragmentation or even to cluster ionization or to emission of electrons (see [7] and references given in [10]). Experimental studies concerning cluster-ion/surface “reactions” have been mainly restricted to SID reactions (see references in [11] and some early examples [12]), nevertheless including in the case of singly-charged fullerene ions also the observation of surface pick-up reactions [13]. Recently, Cleveland and Landman [14] investigated the structure, energetics and dynamics of shock conditions generated in a nanocluster upon impact on a sodium chloride crystalline surface using molecular dynamics simulations for a 561 atom argon cluster incident with a velocity of 3 km/s (energy of ≈ 1.9 eV per atom). Their findings demonstrated that the impact of this cluster on the surface results in a piling-up phenomenon leading to high-energy collision cascades and the development of a new transient medium in the cluster environment characterized by extreme density, pressure and temperature conditions,

propagating in the cluster in a shock wave-like manner on a time scale of about 1 ps. In their conclusions they suggested that in the presence of reactants embedded in this colliding cluster, such collisions could catalyze chemical reactions between cluster constituents as well as between cluster constituents and the surface material. Moreover, Landman and co-workers [14] argued that because of the highly nonequilibrium nature of this new chemical medium, such reactions may evolve in dynamic and kinetic pathways quite different from those known in equilibrium thermodynamic conditions. In a follow-up paper, Levine and co-workers suggested – based on molecular dynamics calculations – the possible existence of intracluster reactions such as “burning air” in mixed nitrogen/oxygen clusters [15] which definitively would constitute an extension of the processes (1) to (4) summarized above.

Typically, polyatomic ion-surface reactions are studied with a tandem mass spectrometer set-up consisting of a combination of two or more mass analyzers such as a magnetic sector field analyzer (B), a quadrupole mass analyzer (Q) or a time of flight (TOF) analyzer [1, 2, 16]. The first mass analyzer is used to select the primary ion and the second mass analyzer (sometimes complemented by an energy analyzer) is employed to record the secondary mass spectrum as a function of the collision energy (and sometimes as a function of energy and angle). In order to allow a quantitative investigation of SID and SIR processes (for instance to determine activation energies [17]) it is of utmost importance to control and determine accurately the collision energy and to achieve energy spreads as small as possible. So far the best energy resolution achieved for the study of polyatomic ions was a FWHM distribution of about 2–4 eV [17], whereas for cluster ions distributions of several tens of eV FWHM have been the state of the art for the past few years [10, 13, 18].

In a recent effort to improve this situation we have constructed the tandem mass spectrometer set-up BESTOF (consisting of a B-sector field combined with an E-sector field, a Surface and a Time Of Flight mass spectrometer) [11, 19–25] which allows the investigation of ion/surface reactions with high primary mass and energy resolution, i.e., energy spreads of as low as 80 meV FWHM have been achieved. Using BESTOF we have extended previous investigations in several respects [11, 19–25], e.g., we have investigated surface induced reactions (using stainless steel and gold surfaces) of fullerene ions as a function of cluster size n and cluster charge state z (up to $z = 5$) thereby extending the previous measurements of Kappes and co-workers [13] for singly-charged fullerene ions to multiply-charged fullerene ions [25]. The results obtained corroborate measurements carried out in collaboration with Winter and co-workers [26–28] on the electron number statistics (from which total electron yields have been derived) for the impact of slow multiply-charged fullerene ions on an atomically clean polycrystalline gold surface showing as the most surprising result a complete suppression of potential electron emission. In this contribution we will first describe shortly the characteristics of this newly constructed tandem mass spectrometer system BESTOF. We will then discuss results ob-

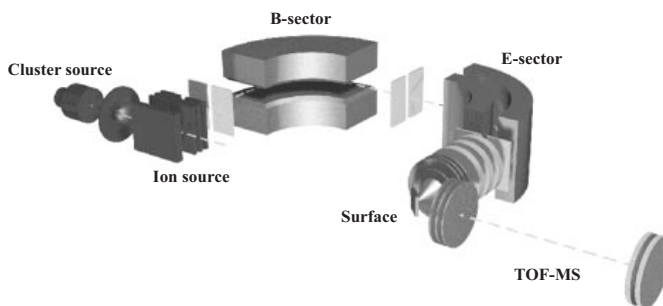


Fig. 1. Schematic view of the experimental apparatus BESTOF.

tained with this machine using the acetone dimer ion as a projectile ion.

2 Experimental

The experimental apparatus BESTOF (see Fig. 1) constructed recently in Innsbruck consists of a double focusing two sector field mass spectrometer (reversed geometry) in combination with a linear time-of flight mass spectrometer. Neutral van der Waals clusters are produced by supersonic expansion through a 20 μm nozzle in a continuous, cooled or heated cluster source. The pressure of the expanding gas can be as high as 2 bar and the temperature in the expansion vessel can be controlled in the range from -180 to 120 $^{\circ}\text{C}$. Alternatively, neutral or ionized metal clusters can be produced by a PACIS (pulsed arc cluster ion source) cluster source [29]. Moreover, a neutral C_{60} beam may be produced by evaporating pure C_{60} powder in a temperature-controlled Knudsen type oven operated typically at around 900 K. After passing through a skimmer the neutral cluster beam or C_{60} beam enters transversely into a Nier-type electron impact ion source. The neutral clusters are ionized by impacting them with electrons whose energy can be varied from below the ionization energy up to about 500 eV.

The ions produced are extracted from the ion source region and accelerated to about 3 keV for mass- and energy-analysis by the double-focusing two-sector-field mass spectrometer. The nominal mass resolution of this two-sector field mass spectrometer exceeds at 3 keV a value of 10 000 and thus allows easily the selection of isotopically pure primary ions. After passing the exit slit of the mass spectrometer, ions are refocused by an Einzel lens and the deceleration optics positioned in front of the stainless steel surface. Field penetration effects are minimized by shielding the surface with conical shield plates. The incident impact angle δ of the primary ions at the surface is usually kept at 45° and the scattering angle is fixed at 90° .

The collision energy of ions impacting on the surface is defined by the potential difference between the ion source and the surface. The potential difference (hence, the collision energy) can be varied from zero to about 2 keV with a typical resolution better than 200 meV. We have determined the energy and energy spread of the primary ion

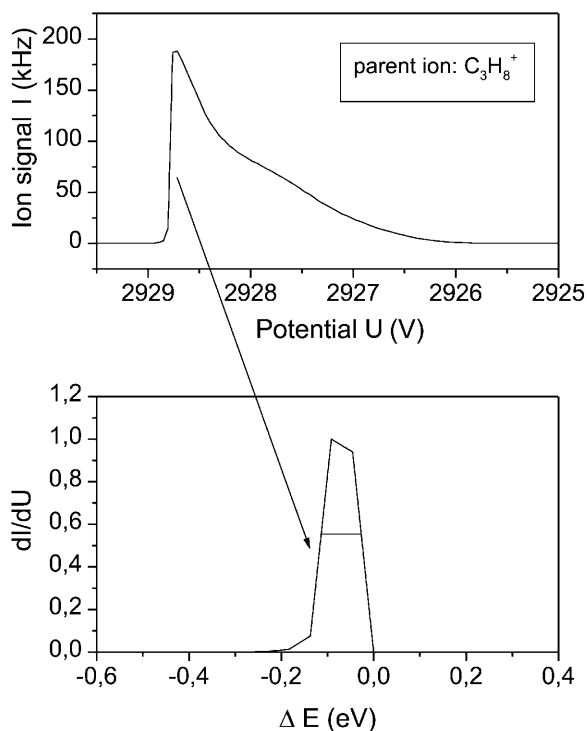


Fig. 2. Total reflected ion current for the surface impact of the propane ion C_3H_8^+ as a function of the nominal retarding potential in the vicinity of the ion acceleration potential of approximately 2929 V (upper panel). The derivative of the leading edge of this total reflected ion shown in the lower panel indicates a fwhm for the primary ion beam spread of about 90 meV.

beam by using the surface as a retarding potential and measuring the (reflected) total ion signal as a function of the surface potential. The energy spread is then given by the FWHM of the first derivative of the total ion signal. Figure 2 shows as an example in the upper panel the total reflected ion current for the impact of the propane ion C_3H_8^+ as a function of the nominal retarding potential in the vicinity of the ion acceleration potential of approximately 2929 V. If the retarding potential is above the acceleration potential no ions will hit the surface and thus no ions will be detected, if the retarding potential is lowered primary ions will start to be able to hit the surface and the reflected ion current will strongly increase to its peak value. The ensuing decrease of the reflected ion current with decreasing retarding potential (amounting to increasing collision energy) is due to the loss of primary ions at the surface via neutralization processes. The derivative of the leading edge of this total reflected ion current shown in the lower panel of Fig. 2 indicates in this case a FWHM for the primary ion beam spread of about 90 meV. This energy spread is caused by the ion production process and the ion extraction from the ion source and can be minimized in the best case to about 80 meV.

A fraction of the secondary ions formed at the surface exits the shielded chamber through a 1 mm diameter orifice. These ions are then subjected to the pulsed extraction and acceleration field which initiates time-of-flight

analysis of these ions. This second mass analyzer is a linear time-of-flight mass selector with a flight tube of about 80 cm in length. The mass selected ions are detected by a double stage multi-channelplate which is connected to a fast scaler (with a time resolution of 5 ns per channel) and a laboratory computer. Mass resolution has been improved steadily the past two years and is to date approximately 100. The present experiments have been carried out using a stainless steel surface under ultra high vacuum conditions (10^{-10} Torr) maintained in our bakeable turbo-pumped surface collision chamber. However, even these conditions do not exclude the production of monolayers of hydrocarbon contaminants (pump oil etc.) on the surface whenever the valve between the mass spectrometers and the surface collision chamber is opened and the pressure in the target region is rising to the 10^{-9} Torr range.

3 Results

The positive ion mass spectrum after ionization of the acetone molecule by 70 eV electrons shows a very simple fragmentation pattern: the most abundant peaks are the fragment ion peak at $m/z = 43$ (CH_3CO^+) and the parent peak at $m/z = 58$ ($\text{CH}_3\text{COCH}_3^+$). All other fragment ions are much less abundant (accounting each to less than 7% of the peak at $m/z = 43$) and are due to CH_i^+ (mass 12, 13, 15), C_2H_i^+ (mass 24–29), $\text{C}_2\text{H}_2\text{O}^+$ (mass 42) and $\text{C}_3\text{H}_i\text{O}^+$ (mass 53, 55, 57, 58). In contrast to the monomer, the positive ion mass spectrum after ionization of an acetone cluster beam by 70 eV electrons shows a more complicated fragmentation pattern: besides the monomer acetone parent ion peak and the various fragment ions (mass 43 and smaller mentioned above), additional series of cluster ions are present such as the stoichiometric cluster ions $(\text{CH}_3\text{COCH}_3)_n^+$, the protonated cluster ions $(\text{CH}_3\text{COCH}_3)_n\text{H}^+$ and the acetylated ion series $(\text{CH}_3\text{COCH}_3)_n\text{CH}_3\text{CO}^+$. The mass spectrum is dominated by the stoichiometric cluster ion series, but the abundance of the non-stoichiometric ions – which are readily identified as ion-molecule reaction products in the acetone system – is of the same order of magnitude.

It is interesting to note that the ratio of the abundance of the two non-stoichiometric cluster ions $(\text{CH}_3\text{COCH}_3)_n\text{H}^+ / (\text{CH}_3\text{COCH}_3)_n\text{CH}_3\text{CO}^+$ is 1.5, similar to the ratio of the analogous products formed in the gas phase via reactions of the acetone parent cation with the neutral acetone molecule [30–32]. Thus these ions are formed, in analogy to the gas-phase, by exothermic intra-cluster ion molecule reactions of acetone molecular ions with neighbouring acetone molecules in the cluster, the ions being initially generated by electron impact ionization of neutral clusters. Because of subsequent stabilizing monomer evaporations the ensuing final cluster ion size is usually considerably smaller than that of the initial neutral cluster hit by the electron [33]. Nevertheless, in the present investigation we will only concentrate on the interaction of the stoichiometric dimer ion with the hydrocarbon covered stainless steel sur-

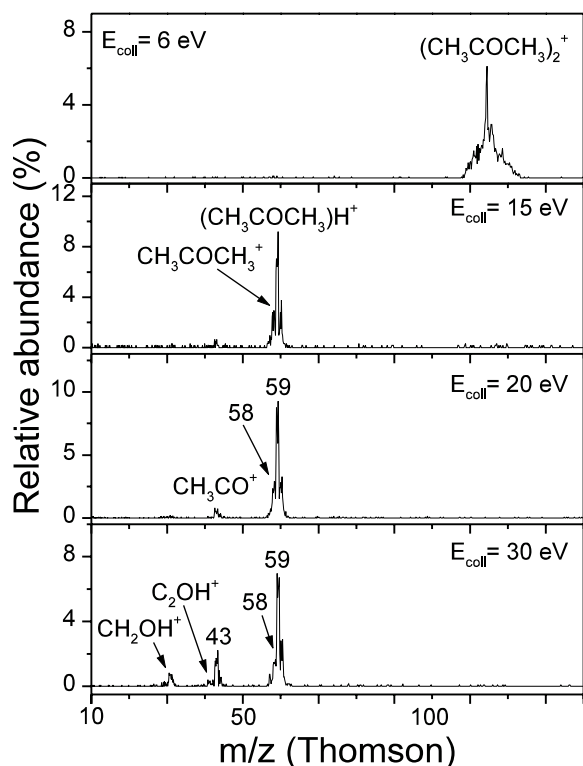


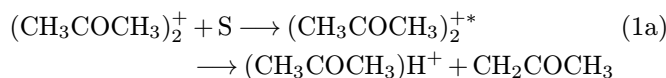
Fig. 3. Secondary mass spectra for the impact of the acetone dimer ion $(\text{CH}_3\text{COCH}_3)_2^+$ for different collision energies.

face. For further results see forthcoming papers from our laboratory [23, 34].

Figure 3 illustrates the surface collision reaction products for the impact of mass selected dimer ions $(\text{CH}_3\text{COCH}_3)_2^+$ at the collision energy of 6, 15, 20 and 30 eV. In line with the results for other polyatomic ions [1, 2, 11, 19–22], interaction of the acetone dimer ion with a surface at very low collision energies only leads to the reflection of the projectile dimer ion (see Fig. 3, top panel), the absolute abundance drastically decreasing with increasing collision energy due to neutralisation reactions. Above a certain collision energy of about 7 eV the total ion current is increasing due to the increased production of product ions. At around 20 eV the major secondary ions are (i) the protonated monomer ion $(\text{CH}_3\text{COCH}_3)\text{H}^+$, which was already noted to be a major intra-cluster ion-molecule reaction product in the case of electron impact ionization of neutral acetone clusters, and (ii) the monomer ion $(\text{CH}_3\text{COCH}_3)^+$ very likely arising from the simple collision induced decomposition of the dimer projectile ion. Both types of product ions are observed at collision energies as low as 10 eV. The abundance of the acetyl cation, which is a minor fragment secondary ion at 20 eV, increases monotonically with collision energy. The acetyl ion is the major collision-induced decomposition product for the acetone molecular ion in the gas phase [35]; it is also a major dissociation product formed in electron impact ionization (see above) and low energy surface-induced reaction upon impact of the acetone molecular ion on a surface [19]. Consequently, we identify the acetyl cation with the breakup

of molecular acetone ions after surface impact of the dimer ion. In addition to the acetyl ion several fragment ions, CH_3^+ and CH_2OH^+ (and to a minor extent C_2OH^+), are observed in appreciable amounts at higher collision energies. CH_3^+ is known to be a fragment ion of the acetone monomer ion (similar to the acetyl case, see above), whereas the CH_2OH^+ ion is known [19] to be a secondary dissociation product of protonated acetone cations (produced by surface pick-up reactions of the acetone monomer ion in surface collisions) when the collision energy is increased. As both, the acetone monomer ion and the protonated acetone ion are present in the present secondary mass spectrum and both are decreasing in relative abundance as the other fragment ions, i.e., CH_3^+ , CH_2OH^+ and CH_3CO^+ , are increasing in relative abundance with increasing collision energy, the production pathways of these fragment ions appear to be straightforward. As will be discussed below, the production route(s) of the protonated acetone monomer ion, however, is the real interesting point in this study.

As discussed above, surface reactions and decomposition of the acetone monomer cation gives as a major product ion the protonated acetone ion formed exclusively by H-abstraction from hydrocarbons chemisorbed on the surface [19]. As shown in Fig. 3, this protonated acetone ion is also the most prominent reaction product from the surface reaction of acetone dimer ions (and also for higher cluster analogues discussed in [23, 34]). Thus in line with the aforementioned it is conceivable that in principle this ion may be produced by two competing reactions by the impacting dimer ion, i.e.,



where reaction (1a) represents a surface collisional activation of the impinging dimer ion followed by an intra-cluster ion molecule reaction between the acetone ion and its neighbouring neutral molecule (discussed already in the context of electron impact ionization of neutral acetone clusters, see above) and reaction (1b) represents a reaction with surface hydrogen containing adsorbates (dissociative H-pick-up reaction).

Important insight into the origin of the protonated acetone formation can be gained by performing an additional experiment using completely deuterated acetone dimer ions $(\text{CD}_3\text{COCD}_3)_2^+$ as projectiles. Preliminary results indicate in this case, that the monomer ion group in the secondary ion mass spectrum consists of three peaks, corresponding to the deuterated acetone ion $(\text{CD}_3\text{COCD}_3)\text{D}^+$, the protonated acetone ion $(\text{CD}_3\text{COCD}_3)\text{H}^+$, and the acetone monomer 'fragment' ion $\text{CD}_3\text{COCD}_3^+$. It is clear, that in this case the deuterated acetone ion is produced in analogy to reaction (1a) via a *surface induced intra-cluster ion molecule reaction*, whereas the protonated acetone ion is produced in analogy

to reaction (1b) via a reaction of the impinging dimer ion with hydrogen containing surface adsorbates.

In order to rationalize the occurrence of these reaction products for the interaction of the acetone dimer ion with the surface, we have to assume that the hydrogen-bonded dimer ion may alternatively exist before the impact in two different isomeric configurations separated by a small barrier (for details see [23]), i.e., one consisting of $(\text{CD}_3\text{COCD}_2)(\text{CD}_3\text{COCD}_3)\text{D}^+$ and one consisting of $(\text{CD}_3\text{COCD}_3)(\text{CD}_3\text{COCD}_3)^+$. Surface collisions convert translational energy very efficiently into internal energy [1]. For the present example, the sudden increase in internal energy results in dissociation with localization of the charge on either the deuterated acetone structure $(\text{CD}_3\text{COCD}_3)\text{D}^+$ or on the molecular ion $(\text{CD}_3\text{COCD}_3)^+$. Similar to the monomer case [19], in the latter case most of the molecular acetone cations may then react with surface hydrocarbons to give by hydrogen abstraction protonated acetone $(\text{CD}_3\text{COCD}_3)\text{H}^+$ as its major product. The intact molecular ion $(\text{CD}_3\text{COCD}_3)^+$, is also observed as a less abundant dissociation product. Some of those ions may be ions which after dissociation at the surface have not reacted to $(\text{CD}_3\text{COCD}_3)\text{H}^+$, but some of those ions may also have been formed in slow dissociations of the receding dimer ion to $(\text{CD}_3\text{COCD}_3)^+ + (\text{CD}_3\text{COCD}_3)$, after the interaction with the surface.

In conclusion, we have here extended previous studies about the interaction of an acetone monomer ion with a hydrocarbon covered stainless steel surface [19] to studies concerning surface induced reactions of the acetone dimer ion. In particular, we have been able - as predicted by Cleveland and Landman [14] (see also [15, 36–39]) using molecular-dynamics simulations - to observe here besides surface induced dissociation (SID) also surface induced reactions (SIR) of acetone dimer ions upon impact on a hydrocarbon covered stainless steel surface. Using fully deuterated acetone dimer ions we obtained evidence for the occurrence of two competing surface-induced reactions, i.e., on the one hand intra-cluster ion molecule reactions leading to the production of the deuterated acetone monomer ion $(\text{CD}_3\text{COCD}_3)\text{D}^+$ and on the other hand hydrogen pick-up reactions leading to the formation of the protonated acetone monomer ion $(\text{CD}_3\text{COCD}_3)\text{H}^+$.

Work supported by FWF, ÖAW/EURATOM, ÖNB, BMWV, Wien, Austria. It is a pleasure to thank Prof. Zdenek Herman, Praha, Prof. Helmut Schwarz, Berlin and Prof. Jean Futrell, Delaware.

References

1. R.G. Cooks, T. Ast, M.A. Mabud: *Int. J. Mass Spectrom. Ion Processes* **100**, 209 (1990); A. Amirav: *Comments At. Mol. Phys.* **24**, 187 (1990)
2. L. Hanley (Ed.): *Special issue on Polyatomic ion-surface interactions*, *Int. J. Mass Spectrom.* **174** (1998)
3. W.O. Hofer, J. Roth (Eds.): *Physical Processes of the Interaction of Fusion Plasmas with Solids* (Academic Press, San Diego 1996)
4. J.P. Booth: *Proc. XIVth European Sectional Conference Atomic and Molecular Physics in Ionized Gases (ES-CAMPIG)*, Malahide, Ireland (1998)
5. D.B. Graves, M.J. Kushner, J.W. Gallagher, A. Garscaden, G.S. Oehrlein, A.V. Phelps: *Database needs for modeling and simulation of plasma processing*, Report by the panel on database needs in plasma processing (National Research Council, National Academy Press, Washington, DC 1996)
6. R.K. Janev (Ed.): *Atomic and Molecular Processes in Fusion Edge Plasmas* (Plenum, New York 1995)
7. S. Matt, T.D. Märk, K.H. Meiwes-Broer (Eds.): *Cluster Surface Interactions*, Book of Abstracts of ESF Conference, Cargese, Corse (1998)
8. T.D. Märk, A.W. Castleman: *Adv. Atom. Molec. Phys.* **20**, 66 (1985)
9. H. Haberland (Ed.): *Clusters of Atoms and Molecules I and II* (Springer, Berlin 1994)
10. W. Christen, U. Even, T. Raz, R.D. Levine: *Int. J. Mass Spectrom.* **174**, 35 (1998)
11. V. Grill, R. Wörgötter, J.H. Futrell, T.D. Märk: *Z. Phys. D* **40**, 111 (1997)
12. R.D. Beck, P.S. John, M.M. Alvarez, F. Diederich, R.L. Whetten: *J. Phys. Chem.* **95**, 8402 (1991); H.G. Busmann, T. Lill, B. Reif, I.V. Hertel: *Surf. Sci.* **272**, 146 (1992); H. Yasumatsu, U. Kalmbach, S. Koizumi, A. Terasaki, T. Kondow: in *Structure and Dynamics of Clusters*, ed. by T. Kondow, K. Kaya, A. Terasaki (Universal Academy Press, Tokyo 1996) pp. 485
13. R.D. Beck, J. Rockenberger, P. Weis, M.M. Kappes: *J. Chem. Phys.* **104**, 3638 (1996)
14. C.L. Cleveland, U. Landman: *Science* **257**, 355 (1992)
15. T. Raz, R.D. Levine: *Chem. Phys. Lett.* **246**, 405 (1995)
16. V. Grill, R.G. Cooks: *Contributions to Symposium on Atomic and Surface Physics SASP 98*, ed. by A. Hansel, W. Lindinger, (Going 1998) p. 129
17. S.B. Wainhaus, E.A. Gislason, L. Hanley: *J. Am. Chem. Soc.* **119**, 4001 (1997)
18. T.M. Bernhardt, B. Kaiser, K. Rademann: *Z. Phys. Chem.* **195**, 273 (1996); *Z. Phys. D* **40**, 327 (1997); B. Kaiser, T.M. Bernhardt, K. Rademann: *Nucl. Instrum. Methods Phys. Res. B* **125**, 223 (1997)
19. R. Wörgötter, V. Grill, Z. Herman, H. Schwarz, T.D. Märk: *Chem. Phys. Lett.* **270**, 333 (1997)
20. R. Wörgötter, C. Mair, T. Fiegele, V. Grill, T.D. Märk, H. Schwarz: *Int. J. Mass Spectrom. Ion Processes* **164**, L1 (1997)
21. R. Wörgötter, J. Kubista, J. Zabka, Z. Dolejšek, T.D. Märk, Z. Herman: *Int. J. Mass Spectrom.* **174**, 53 (1998)
22. C. Mair, T. Fiegele, R. Wörgötter, J.H. Futrell, T.D. Märk: *Int. J. Mass Spectrom. Ion Processes* **177**, 105 (1998)
23. C. Mair, Z. Herman, T. Fiegele, J.H. Futrell, T.D. Märk: *Int. J. Mass Spectrom.* **188**, 21 (1999)
24. C. Mair, T. Fiegele, F. Biasioli, T.D. Märk, W.R. Hess: *International Congress on Plasma Physics*, Book of Abstracts, ed. by J. Badalec, J. Stöckel, P. Sunka, M. Tendler, Prague (1998) p. 171
25. T. Fiegele, F. Biasioli, C. Mair, T.D. Märk, F. Aumayr, G. Betz, HP. Winter: *Book of Abstracts ERC Symposium on Cluster surface interaction*, ed. by S. Matt, T.D. Märk, K.H. Meiwes-Broer, Cargese (1998) p. 63
26. K. Tögelhofer, F. Aumayr, H. Kurz, HP. Winter, P. Scheier, T.D. Märk: *J. Chem. Phys.* **99**, 8254 (1993)

27. HP. Winter, M. Vana, G. Betz, F. Aumayr, H. Drexel, P. Scheier, T.D. Märk: *Phys. Rev. A* **56**, 3007 (1997)
28. F. Aumayr, M. Vana, HP. Winter, H. Drexel, V. Grill, G. Senn, S. Matt, P. Scheier, T.D. Märk: *Int. J. Mass Spectrom. Ion Processes* **163**, L9 (1997)
29. H.R. Siekmann, C. Lüder, J. Faehrmann, H.O. Lutz, K.H. Meiwes-Broer: *Z. Phys. D* **20**, 417 (1991)
30. K.A.G. McNeil, J.H. Futrell: *J. Phys. Chem.* **76**, 409 (1972)
31. A.S. Blair, A.G. Harrison: *Can. J. Chem.* **51**, 703 (1973)
32. M. Kumakura, T. Sufura: *J. Phys. Chem.* **82**, 639 (1978)
33. T.D. Märk: in *Linking the Gaseous and Condensed Phases of Matter*, ed. by L.G. Christophorou, E. Illenberger, W.F. Schmidt (Plenum Press, New York 1994) pp. 155
34. C. Mair, T. Fiegele, F. Biasioli, Z. Herman, T.D. Märk: *J. Chem. Phys.* **111**, 2770 (1999)
35. J.H. Futrell: private communication (1998)
36. U. Even, I. Schek, J. Jortner: *Chem. Phys. Lett.* **202**, 303 (1993)
37. T. Raz, I. Schek, M. Ben-Nun, U. Even, J. Jortner, R.D. Levine: *J. Chem. Phys.* **101**, 8606 (1994)
38. I. Schek, T. Raz, R.D. Levine, J. Jortner: *J. Chem. Phys.* **101**, 8596 (1994)
39. I. Schek, J. Jortner, T. Raz, R.D. Levine: *Chem. Phys. Lett.* **257**, 273 (1996)